

 Open access • Journal Article • DOI:10.1109/TMTT.2012.2202685

## Variability Analysis of Multiport Systems Via Polynomial-Chaos Expansion

— [Source link](#) 

Domenico Spina, Francesco Ferranti, Tom Dhaene, Luc Knockaert ...+2 more authors





**Institutions:** Ghent University

**Published on:** 19 Jun 2012 - IEEE Transactions on Microwave Theory and Techniques (IEEE)

**Topics:** Polynomial chaos

Related papers:

- [The Wiener--Askey Polynomial Chaos for Stochastic Differential Equations](#)
- [Stochastic Analysis of Multiconductor Cables and Interconnects](#)
- [Decoupled Polynomial Chaos and Its Applications to Statistical Analysis of High-Speed Interconnects](#)
- [Stochastic Modeling-Based Variability Analysis of On-Chip Interconnects](#)
- [Stochastic Testing Method for Transistor-Level Uncertainty Quantification Based on Generalized Polynomial Chaos](#)

Share this paper:    

View more about this paper here: <https://typeset.io/papers/variability-analysis-of-multiport-systems-via-polynomial-2hs3s2j3w6>

# Variability Analysis of Multiport Systems via Polynomial Chaos Expansion

Domenico Spina, Francesco Ferranti, *Member, IEEE*, Tom Dhaene, *Senior Member, IEEE*,  
 Luc Knockaert, *Senior Member, IEEE*, Giulio Antonini, *Senior Member, IEEE*,  
 Dries Vande Ginste, *Member, IEEE*

**Abstract**—We present a novel technique to perform variability analysis of multiport systems. The versatility of the proposed technique makes it suitable for the analysis of different types of modern electrical systems (e.g. interconnections, filters, connectors). The proposed method, based on the calculation of a set of univariate macromodels and on the use of the Polynomial Chaos expansion, produces a macromodel of the transfer function of the multiport system including its statistical properties. The accuracy and the significant speed-up with respect to the classical Monte Carlo analysis are verified by means of two numerical examples.

**Index Terms**—Multiport systems, variability analysis, polynomial chaos, rational modeling.

## I. INTRODUCTION

The increasing demand for performance from integrated circuits (ICs) pushes operation to higher signal bandwidths, while rapid advances in manufacturing capabilities have significantly reduced the feature size and increased the density of these devices. In this scenario, the analysis of the effects of geometrical or electrical parameters variability on the ICs performance is fundamental.

The standard approach for variability analysis is the Monte Carlo (MC) method. MC gives accurate results and its implementation is straightforward, but it requires a large number of simulations. Since simulations are often computationally expensive due to the increased complexity of systems, MC has a very high computational cost. Recently, a new approach, based on the Polynomial Chaos (PC) expansion, has emerged to perform variability analysis as an efficient alternative to the computationally cumbersome MC-based techniques. The PC-based modeling approach expands a stochastic process in terms of orthogonal polynomials, giving an analytical representation of the variability of the system with respect to the random variables under consideration [1]. Over the recent years, techniques were developed to study the stochastic variations of electrical circuits by means of the PC expansion.

Domenico Spina, Francesco Ferranti, Tom Dhaene and Luc Knockaert are with the Department of Information Technology, Internet Based Communication Networks and Services (IBCN), Ghent University – IBBT, Gaston Crommenlaan 8 Bus 201, B-9050 Gent, Belgium, email: {domenico.spina, francesco.ferranti, tom.dhaene, luc.knockaert}@intec.ugent.be;

Dries Vande Ginste is with the Department of Information Technology, Electromagnetics Group, Ghent University, Sint-Pietersnieuwstraat 41, B-9000 Gent, Belgium, email: dries.vandeginste@intec.Ugent.be;

Giulio Antonini is with the UAq EMC Laboratory, Dipartimento di Ingegneria Elettrica e dell'Informazione, Università degli Studi dell'Aquila, Via G. Gronchi 18, 67100, L'Aquila, Italy, phone: +390862434462, email: giulio.antonini@univaq.it.

These techniques were tailored to handle specific systems, namely multiconductor transmission lines [2]–[4] and lumped elements circuits [5], [6].

Instead, the variability analysis technique presented in this paper can be applied to any generic multiport system, if the linear system can be described by a state-space model. The starting point of the proposed technique is the evaluation of the system transfer function on a discrete set of frequencies and geometrical or physical parameters chosen for the variability analysis. The transfer function of the system in the frequency-domain can be expressed in different forms (e.g. scattering, impedance or admittance parameters), making the proposed method applicable to a large range of microwave systems. Next, a univariate frequency-domain macromodel is computed using the Vector Fitting (VF) technique [7] – [9] for each combination of the discretized design parameters. In this paper, we refer to these initial univariate macromodels as *root macromodels*. Afterwards, a state-space realization is obtained for each *root macromodel*, allowing to calculate the PC model with respect to the random variables under consideration.

The main advantage of this new approach is clear: the PC-model of the state-space matrices is able to describe the statistical properties of the system over the entire frequency range of the chosen samples. Furthermore, the PC model of the system transfer function can be calculated for each frequency of interest by combining the PC model of the state-space matrices with the existing deterministic equations for systems expressed in state-space form. Finally, the corresponding PC expansion of the ports voltage and current can be easily obtained from the PC representation of the system transfer function.

This paper is structured as follows. First, an overview of PC theory is given in Section II. The variability analysis in the frequency-domain is described in Section III, and two pertinent numerical microwave examples are presented in Section IV, validating the proposed technique. Conclusions are summed up in Section V.

## II. PRELIMINARIES: PC PROPERTIES

Under specific conditions [10], a stochastic process  $Y$  can be expanded as a series of orthogonal polynomials with suitable coefficients as [1]

$$Y = \sum_{i=0}^{\infty} \alpha_i \varphi_i(\boldsymbol{\xi}) \quad (1)$$

where  $\varphi_i(\boldsymbol{\xi})$  are the corresponding orthogonal polynomials depending on the vector of normalized random variables  $\boldsymbol{\xi}$  and the coefficients  $\alpha_i$  are called PC coefficients. Regarding the polynomials, the following orthogonality condition is satisfied [11]

$$\langle \varphi_i(\boldsymbol{\xi}), \varphi_j(\boldsymbol{\xi}) \rangle = \int_{\Omega} \varphi_i(\boldsymbol{\xi}) \varphi_j(\boldsymbol{\xi}) W(\boldsymbol{\xi}) d\boldsymbol{\xi} = a_i \delta_{ij} \quad (2)$$

where  $a_i$  are positive numbers,  $\delta_{ij}$  is the Kronecker delta and  $W(\boldsymbol{\xi})$ , called weighting function in the theory of orthogonal polynomials [12], is a probability measure with support  $\Omega$ . The construction of the PC expansion (1) entails a three-step process:

- Calculating the orthogonal polynomials  $\varphi_i(\boldsymbol{\xi})$ .
- Truncating the series to a finite order.
- Computing the PC coefficients  $\alpha_i$ .

If the stochastic process  $Y$  is composed of independent random variables, the identification of the orthogonal polynomials, also called basis functions, is straightforward: the global uncertainty probability density function (PDF) is the product of the PDFs of the single random variables. In this case, the weighting function can be written as

$$W(\boldsymbol{\xi}) = \prod_{i=1}^N W_i(\xi_i) \quad (3)$$

where  $N$  is the number of random variables. Therefore, due to the orthogonality relation (2), the basis functions  $\varphi_i(\boldsymbol{\xi})$  can be calculated as product combinations of orthogonal polynomials corresponding to each individual random variable  $\xi_i$  [13]. Consequently, (1) can be truncated to a limited number of  $M$  basis functions as

$$\varphi_j(\boldsymbol{\xi}) = \prod_{k=1}^N \phi_{i_k}(\xi_k) \quad \text{with} \quad \sum_{k=1}^N i_k \leq P \quad \text{and} \quad 0 \leq j \leq M \quad (4)$$

where  $\phi_{i_k}(\xi_k)$  represent the polynomial function of degree  $i$  corresponding to the random variable  $\xi_k$  and  $P$  is the highest degree of the polynomials used in the truncated PC expansion. It is easy to show [1] that the total number of basis functions  $M + 1$  used in the PC expansion is

$$M + 1 = \frac{(N + P)!}{N!P!} \quad (5)$$

Note that for random variables with specific PDFs (indicated in the sequel as standard distributions) the basis functions are the polynomials of the Wiener-Askey scheme [12]. For example, in the Gaussian PDF case the basis functions are the Hermite polynomials, and in the uniform PDF case the basis functions are the Legendre polynomials. The optimality of the polynomials of the Wiener-Askey scheme is guaranteed as their weighting function  $W(\boldsymbol{\xi})$  corresponds to the PDF of the associated random variable, when placed in a standard form [11], [12]. Due to this property, an exponential convergence rate can be achieved [11]. Furthermore, optimal basis functions can be calculated numerically for independent random variables with arbitrary PDFs following the approach described in [11].

In the general case of correlated random variables with arbitrary PDFs, the basis functions can be calculated following the approach described in [1], [11], [13]. In this case, decorrelation can be obtained via a variable transformation, such as the Nataf transformation [14] or the Karhunen-Loève expansion [15] and the convergence rate of the PC expansion may not be exponential.

After determination of the basis functions, (1) is truncated as follows

$$Y \approx \sum_{i=0}^M \alpha_i \varphi_i(\boldsymbol{\xi}) \quad (6)$$

Next, the  $M + 1$  PC coefficients  $\alpha_i$  must be computed. Therefore, expressing a stochastic process through the PC expansion requires the calculation of suitable scalar coefficients  $\alpha_i$  for known basis functions.

As pointed out in the previous Section, the main advantage of the PC expansion is the analytical representation of the system variability. For example, the mean  $\mu$  and the variance  $\sigma^2$  of the stochastic process  $Y$  can be written as [1]

$$\mu = \alpha_0 \quad (7)$$

$$\sigma^2 = \sum_{i=1}^M \alpha_i^2 \langle \varphi_i(\boldsymbol{\xi}), \varphi_i(\boldsymbol{\xi}) \rangle \quad (8)$$

Apart from all moments, also stochastic functions of  $Y$ , such as the PDF and the cumulative density function (CDF), can be computed following standard analytical formulas or numerical schemes [16].

If the stochastic process under study is written in a matrix form  $\mathbf{Y}$ , the PC coefficient must be calculated for each entry of  $\mathbf{Y}$ . In this case, (6) can be written as

$$\mathbf{Y} \approx \sum_{i=0}^M \boldsymbol{\alpha}_i \varphi_i(\boldsymbol{\xi}) \quad (9)$$

where  $\boldsymbol{\alpha}_i$  is the matrix of PC coefficients for the  $i$ -th polynomial basis and has the same size of  $\mathbf{Y}$ . For a complete reference to polynomial chaos theory, the reader is referred to [1], [10] – [12].

### III. VARIABILITY ANALYSIS OF MULTIPOINT SYSTEMS

#### A. Transfer function PC modeling

The starting point of our approach is the description of a multipoint system with a generic linear input-output representation in state-space form:

$$(s\mathbf{I} - \mathbf{A}(\boldsymbol{\xi})) \mathbf{X}(s, \boldsymbol{\xi}) = \mathbf{B}(\boldsymbol{\xi}) \quad (10)$$

$$\mathbf{Y}(s, \boldsymbol{\xi}) = \mathbf{C}(\boldsymbol{\xi}) \mathbf{X}(s, \boldsymbol{\xi}) + \mathbf{D}(\boldsymbol{\xi}) \quad (11)$$

where the dependency on a vector of random variables  $\boldsymbol{\xi}$  is explicitly indicated. The goal is to calculate the PC expansion in the form (9) of the state-space variables  $\mathbf{X}$  and, consequently, of the output  $\mathbf{Y}$ , starting from the PC expansion of the state-space matrices. Without loss of generality, for ease of notation, the random variables of the stochastic process  $\mathbf{Y}$  are chosen as independent and the corresponding PDFs are standard distributions. Note, however, that (10) and (11) can also be calculated for the general case of correlated random

variables with arbitrary distributions, using the techniques described in Section II.

In what follows, we will demonstrate that, to achieve our goal, it is necessary to:

- Decide on the number of basis functions  $M$  (5).
- Compute the PC coefficients of the state-space matrices.
- Calculate and solve an equivalent linear system for the coefficients of the PC expansion of  $X$ .
- Combine the obtained results in a suitable way in order to obtain the PC expansion of  $Y$ .

In our approach, the number of basis functions  $M$  is chosen upfront, based on the consideration that, for practical applications,  $P$  can be limited between two and five [2], [12].

Two main approaches exist in the literature to compute the PC coefficients: the spectral projection and the linear regression technique [1]. The first approach projects the stochastic process on each basis function, requiring the evaluation of the following multidimensional integral

$$\alpha_i = \frac{1}{\langle \varphi_i(\boldsymbol{\xi}), \varphi_i(\boldsymbol{\xi}) \rangle} \int_{\Omega} Y(\boldsymbol{\xi}) \varphi_i(\boldsymbol{\xi}) W(\boldsymbol{\xi}) d\boldsymbol{\xi} \quad (12)$$

for each coefficient of the PC expansion.

The second approach calculates all the PC coefficients solving a least-square system [1]

$$\boldsymbol{\Psi} \boldsymbol{\alpha} = \boldsymbol{R} \quad (13)$$

Equation (13) is calculated with respect to an initial set of discrete samples of the normalized random variables  $\boldsymbol{\xi}$ , indicated as  $[\boldsymbol{\xi}_j]_{j=1}^K$ . The  $j$ -th row of the matrix  $\boldsymbol{\Psi}$  contains the multivariate polynomial basis evaluated at  $\boldsymbol{\xi}_j$  and the matrix  $\boldsymbol{R}$  represents the corresponding set of stochastic process values.

To apply the linear regression approach in our method, the equivalent matrices  $\boldsymbol{\Psi}$  and  $\boldsymbol{R}$  must be built for the state-space matrices in (10), (11). The proposed technique starts by computing  $K$  univariate frequency-domain macromodels, called *root macromodels* [17], [18]. This is done by invoking the VF algorithm  $K$  times, i.e., for a discrete set of values of the normalized random variables  $[\boldsymbol{\xi}_j]_{j=1}^K$ , each time using  $L$  frequency samples  $[f_i]_{i=1}^L$ . A simple pole-flipping scheme is used to enforce stability [7]. Afterwards, a state-space realization is obtained for each stable *root macromodel*  $[\boldsymbol{A}_j, \boldsymbol{B}_j, \boldsymbol{C}_j, \boldsymbol{D}_j]_{j=1}^K$  using a realization technique. The realization technique used to convert a pole-residue model to a state-space form has an influence on the smoothness of the state-space matrices with respect to the design parameters and, therefore, on the accuracy of the final PC model. We use a standard Gilbert realization [19] in our approach.

Note that all  $K$  realizations of all state-space matrices must have the same dimensions to build the matrix  $\boldsymbol{R}$ . This requirement can easily be satisfied if one considers that the range of variation of each random variable is relatively small. Therefore, the VF algorithm is applied first to estimate the maximum number of poles needed for the rational modeling by computing the poles at the corner points of the discrete set of initial data, and afterwards to build the corresponding *root macromodels* using this number of poles. Finally, ordering the basis functions and the state-space matrices computed for

each  $\boldsymbol{\xi}_j$ , an equivalent equation (13) can be obtained for each state-space matrix. Let us suppose that  $T$  poles are needed to build each *root macromodel*, then the matrices  $\boldsymbol{\Psi}$ ,  $\boldsymbol{\alpha}$  and  $\boldsymbol{R}$  of equation (13) calculated for the state-space matrix  $\boldsymbol{A}$  can be written as

$$\boldsymbol{\Psi} = \begin{bmatrix} \varphi_0(\boldsymbol{\xi}_1) & \cdots & \varphi_M(\boldsymbol{\xi}_1) \\ \vdots & \vdots & \vdots \\ \varphi_0(\boldsymbol{\xi}_K) & \cdots & \varphi_M(\boldsymbol{\xi}_K) \end{bmatrix}$$

$$\boldsymbol{\alpha} = \begin{bmatrix} \boldsymbol{A}_0 \\ \vdots \\ \boldsymbol{A}_M \end{bmatrix} \quad (14)$$

$$\boldsymbol{R} = \begin{bmatrix} \boldsymbol{A}(\boldsymbol{\xi}_1) \\ \vdots \\ \boldsymbol{A}(\boldsymbol{\xi}_K) \end{bmatrix}$$

where  $\varphi_i(\boldsymbol{\xi}_j)$  is the product of the identity matrix  $\boldsymbol{I}^{T \times T}$  with the  $i$ -th basis function  $[\varphi_i]_{i=1}^M$  calculated for the  $j$ -th sample of  $[\boldsymbol{\xi}_j]_{j=1}^K$ , the symbol  $\boldsymbol{A}_i$ ,  $i = 0, \dots, M$ , represents the  $i$ -th PC coefficient matrix, while  $\boldsymbol{A}(\boldsymbol{\xi}_j)$  is the  $\boldsymbol{A}$  matrix calculated for  $[\boldsymbol{\xi}_j]_{j=1}^K$ . Equation (13) for the state-space matrices can be solved in a least squares sense using an element-wise, column-wise or matrix-wise approach.

At this point, we have obtained the representation of the state-space matrices in the form (9), using an a priori estimation of the expansion order and the linear regression method to calculate the PC coefficients, which are from now on denoted as  $\boldsymbol{A}_i$ ,  $\boldsymbol{B}_i$ ,  $\boldsymbol{C}_i$ ,  $\boldsymbol{D}_i$ ,  $i = 0, \dots, M$ . Using (9) to express the state-space matrices, the state-vector and the output, (10) and (11) can be rewritten as

$$s \sum_{j=0}^M \boldsymbol{X}_j(s) \varphi_j(\boldsymbol{\xi}) = \sum_{i=0}^M \sum_{j=0}^M \boldsymbol{A}_i \boldsymbol{X}_j(s) \varphi_i(\boldsymbol{\xi}) \varphi_j(\boldsymbol{\xi}) + \sum_{i=0}^M \boldsymbol{B}_i \varphi_i(\boldsymbol{\xi}) \quad (15)$$

$$\sum_{j=0}^M \boldsymbol{Y}_j(s) \varphi_j(\boldsymbol{\xi}) = \sum_{i=0}^M \sum_{j=0}^M \boldsymbol{C}_i \boldsymbol{X}_j(s) \varphi_i(\boldsymbol{\xi}) \varphi_j(\boldsymbol{\xi}) + \sum_{i=0}^M \boldsymbol{D}_i \varphi_i(\boldsymbol{\xi}) \quad (16)$$

where the only unknowns are the matrices of PC coefficients  $\boldsymbol{X}_j(s)$  for the state-vector, and  $\boldsymbol{Y}_j(s)$  for the output. Next we calculate the desired state-vector coefficients solving a corresponding linear system of the form

$$\boldsymbol{\Phi}_X \boldsymbol{X}_\alpha = \boldsymbol{B}_\alpha \quad (17)$$

where  $\boldsymbol{B}_\alpha$  is the matrix containing all PC coefficients of the  $\boldsymbol{B}$  matrix,  $\boldsymbol{X}_\alpha$  is the matrix containing all unknown PC coefficients and  $\boldsymbol{\Phi}_X$  is a matrix containing weighted scalar products as discussed in what follows. Equation (17) can be obtained by projecting (15) on the basis functions of the PC expansion. To explain how (17) is built, let us for simplicity

assume that the state-space matrices depend on one random variable and two basis functions are used for the PC expansion. The extension to the case of multiple random variables and higher order of expansion is straightforward. Furthermore, the explicit dependency on the vector  $\xi$  is omitted in the following equations, for the sake of clarity. In this simplified case, equation (15) can be rewritten as

$$\begin{aligned} s\mathbf{X}_0\varphi_0 + s\mathbf{X}_1\varphi_1 &= \mathbf{A}_0\mathbf{X}_0\varphi_0\varphi_0 \\ &+ \mathbf{A}_1\mathbf{X}_0\varphi_1\varphi_0 + \mathbf{A}_0\mathbf{X}_1\varphi_0\varphi_1 + \mathbf{A}_1\mathbf{X}_1\varphi_1\varphi_1 \\ &+ \mathbf{B}_0\varphi_0 + \mathbf{B}_1\varphi_1 \end{aligned} \quad (18)$$

Due to the orthogonality relation (2), projection of (18) onto the first basis function  $\varphi_0$ , yields

$$\begin{aligned} s\mathbf{X}_0 \langle \varphi_0, \varphi_0 \rangle &= \\ \mathbf{A}_0\mathbf{X}_0 \langle \varphi_0\varphi_0, \varphi_0 \rangle &+ \mathbf{A}_1\mathbf{X}_0 \langle \varphi_1\varphi_0, \varphi_0 \rangle \\ + \mathbf{A}_0\mathbf{X}_1 \langle \varphi_0\varphi_1, \varphi_0 \rangle &+ \mathbf{A}_1\mathbf{X}_1 \langle \varphi_1\varphi_1, \varphi_0 \rangle \\ + \mathbf{B}_0 \langle \varphi_0, \varphi_0 \rangle & \end{aligned} \quad (19)$$

Similarly, projecting (18) onto the second basis function  $\varphi_1$ , we obtain

$$\begin{aligned} s\mathbf{X}_1 \langle \varphi_1, \varphi_1 \rangle &= \\ \mathbf{A}_0\mathbf{X}_0 \langle \varphi_0\varphi_0, \varphi_1 \rangle &+ \mathbf{A}_1\mathbf{X}_0 \langle \varphi_1\varphi_0, \varphi_1 \rangle \\ + \mathbf{A}_0\mathbf{X}_1 \langle \varphi_0\varphi_1, \varphi_1 \rangle &+ \mathbf{A}_1\mathbf{X}_1 \langle \varphi_1\varphi_1, \varphi_1 \rangle \\ + \mathbf{B}_1 \langle \varphi_1, \varphi_1 \rangle & \end{aligned} \quad (20)$$

Upon calculation of the scalar products in (19) and (20), a matrix equation in the form (17) is obtained:

$$\begin{pmatrix} \Phi_{X00} & \Phi_{X01} \\ \Phi_{X10} & \Phi_{X11} \end{pmatrix} \begin{pmatrix} \mathbf{X}_0 \\ \mathbf{X}_1 \end{pmatrix} = \begin{pmatrix} \mathbf{B}_0 \\ \mathbf{B}_1 \end{pmatrix} \quad (21)$$

where

$$\begin{aligned} \Phi_{X00} &= s\mathbf{I} - \mathbf{A}_0 \frac{\langle \varphi_0\varphi_0, \varphi_0 \rangle}{\langle \varphi_0, \varphi_0 \rangle} - \mathbf{A}_1 \frac{\langle \varphi_1\varphi_0, \varphi_0 \rangle}{\langle \varphi_0, \varphi_0 \rangle} \\ \Phi_{X01} &= -\mathbf{A}_0 \frac{\langle \varphi_0\varphi_1, \varphi_0 \rangle}{\langle \varphi_0, \varphi_0 \rangle} - \mathbf{A}_1 \frac{\langle \varphi_1\varphi_1, \varphi_0 \rangle}{\langle \varphi_0, \varphi_0 \rangle} \\ \Phi_{X10} &= -\mathbf{A}_0 \frac{\langle \varphi_0\varphi_1, \varphi_1 \rangle}{\langle \varphi_1, \varphi_1 \rangle} - \mathbf{A}_1 \frac{\langle \varphi_1\varphi_0, \varphi_1 \rangle}{\langle \varphi_1, \varphi_1 \rangle} \\ \Phi_{X11} &= s\mathbf{I} - \mathbf{A}_0 \frac{\langle \varphi_0\varphi_1, \varphi_1 \rangle}{\langle \varphi_1, \varphi_1 \rangle} - \mathbf{A}_1 \frac{\langle \varphi_1\varphi_1, \varphi_1 \rangle}{\langle \varphi_1, \varphi_1 \rangle} \end{aligned} \quad (22)$$

and  $\mathbf{I}$  is the identity matrix. Note that solving (21) for different frequency samples does not require renewed calculation of the scalar products in (22). Finally, it is now possible to directly compute the PC coefficients of the output  $\mathbf{Y}_j(s)$ . Indeed, because of the orthogonality relation (2), projecting equation (16) onto the basis functions  $\varphi_p(\xi)$ ,  $p = 0, \dots, M$ , leads to

$$\begin{aligned} \mathbf{Y}_p(s) \langle \varphi_p(\xi) \rangle^2 &= \\ \sum_{i=0}^M \sum_{j=0}^M \mathbf{C}_i \mathbf{X}_j(s) \langle \varphi_i(\xi)\varphi_j(\xi), \varphi_p(\xi) \rangle &+ \mathbf{D}_p \langle \varphi_p(\xi) \rangle^2 \end{aligned} \quad (23)$$

where all the scalar products were already pre-computed in the previous step in order to build the matrix  $\Phi_X$ .

The proposed PC-based approach aims at performing frequency-domain variability analysis on a large range of

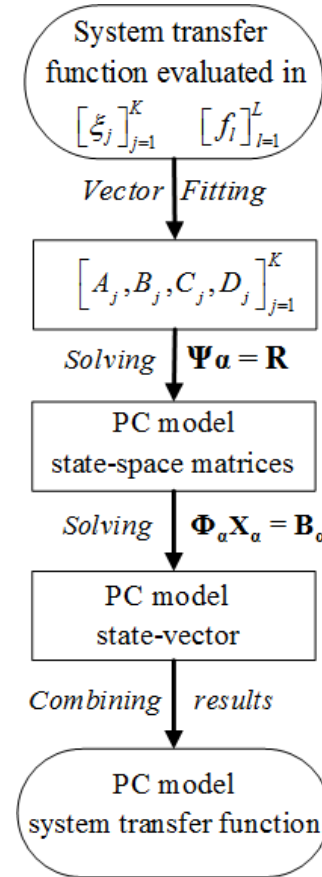


Fig. 1. Flow chart of the proposed modeling strategy.

microwave systems (e.g. filters, connectors, non-uniform transmission lines), overcoming the limitation of the previously developed PC-based technique [2]–[6], that were tailored to handle specific systems. This appealing characteristic of the proposed PC-based method is obtained by applying the PC expansion to a state-space representation of the multiport systems. This approach has two main advantages:

- the system transfer function can be expressed in several forms such as scattering, impedance or admittance parameters;
- the PC model of the state-space representation is frequency independent; however, it allows to describe the system in a large frequency range, see (15), (16).

Indeed, the frequency-dependent PC expansion of the system transfer function can be calculated for every frequency of interest  $f' \in [f_1, f_L]$ , by solving the linear system (17) for  $s = j2\pi f'$  and applying the results obtained in (23). To solve (17), it is only required to compute the projection of (15) onto each basis function. We remark that these projections are frequency-independent and can be calculated upfront. The proposed modeling strategy is summarized in Fig. 1.

### B. Port Voltages and Currents PC modeling

In this Section, we describe how to compute the PC expansion of the port voltages and currents starting from the PC expansion of the transfer function of the multiport system. We

suppose that the terminations are linear and independent of the random variables  $\xi$ . For ease of notation, the dependency on the Laplace variable  $s$  and the random variables  $\xi$  are omitted in the following equations. For a multiport system described by its impedance parameters  $Z$ , the following relation applies [20]:

$$\tilde{V} = Z\tilde{I} \quad (24)$$

where the symbol  $\tilde{V}$  is used for the port voltages and  $\tilde{I}$  for the port currents. We introduce the terminations of the lines to solve (24). In case of linear loads, we have

$$\tilde{I} = I_s - G\tilde{V} - sC\tilde{V} \quad (25)$$

where  $I_s$  is the vector of the source currents, while the matrices  $G$  and  $C$  describe linear resistive and capacitive lumped elements at the ports of the system. Substituting (25) in (24) gives

$$\tilde{V} + Z(G + sC)\tilde{V} = ZI_s \quad (26)$$

In (26) only  $Z$  and  $\tilde{V}$  depend on the random variables  $\xi$  and therefore application of the PC expansion leads to

$$\begin{aligned} \sum_{i=0}^M \tilde{V}_i \varphi_i(\xi) + \sum_{i=0}^M \sum_{j=0}^M Z_j (G + sC) \tilde{V}_i \varphi_i(\xi) \varphi_j(\xi) = \\ \sum_{j=0}^M Z_j I_s \varphi_j(\xi) \end{aligned} \quad (27)$$

where  $\tilde{V}_i$  represents the vector containing the  $i$ -th PC coefficients of the port voltages and  $Z_j$  is a matrix containing the  $j$ -th PC coefficients of the impedance parameters. The desired PC coefficients for the port voltages are again obtained by projecting equation (27) onto the basis functions  $\varphi_p(\xi)$ ,  $p = 0, \dots, M$ , as follows:

$$\begin{aligned} \tilde{V}_p \langle \varphi_p(\xi), \varphi_p(\xi) \rangle + \\ \sum_{i=0}^M \sum_{j=0}^M Z_j (G + sC) \tilde{V}_i \langle \varphi_i(\xi) \varphi_j(\xi), \varphi_p(\xi) \rangle = \\ Z_p I_s \langle \varphi_p(\xi), \varphi_p(\xi) \rangle \end{aligned} \quad (28)$$

As before, the scalar products are already known, because they were pre-computed during the calculation of the matrix  $\Phi_X$ . Therefore, the  $p$ -th PC coefficient vector of the port voltages can be calculated immediately from (28). Once the PC expansion for the port voltages is calculated, the corresponding expression for the port currents can be obtained directly expressing (25) with respect to the chosen basis functions, as follows:

$$\sum_{i=0}^M \tilde{I}_i \varphi_i(\xi) = I_s - \sum_{i=0}^M G \tilde{V}_i \varphi_i(\xi) - s \sum_{i=0}^M C \tilde{V}_i \varphi_i(\xi) \quad (29)$$

Similar relations apply in the case of admittance and scattering parameters, as illustrated in the next Section.

## IV. NUMERICAL EXAMPLES

In this Section, the proposed technique is applied to two different structures. In each example, the scattering parameters of the structure, calculated with respect to a reference impedance of 50  $\Omega$ , are considered as a stochastic process with respect to two or three independent random variables ( $N = 2$  or  $N = 3$ ) with uniform PDFs. The corresponding basis functions are products of the Legendre polynomials [13] and are shown in Table I<sup>1</sup> for  $M = 5$  and  $P = 2$ , while the weighting function (3) is

$$W(\xi) = \begin{cases} 2^{-N}, & |\xi_i| \leq 1, \quad i = 1, \dots, N \\ 0, & \text{elsewhere} \end{cases} \quad (30)$$

The proposed PC-based method and the MC method are compared to validate the efficiency and accuracy of our novel technique. In each example, the scalar products in (17) are calculated analytically on beforehand. The simulations are performed with MATLAB<sup>2</sup> 2010a on a computer with an Intel(R) Core(TM) i3 processor and 4 GB RAM.

TABLE I  
LEGENDRE POLYNOMIALS PRODUCTS FOR TWO INDEPENDENT RANDOM VARIABLES, WITH  $M = 5$  AND  $P = 2$  [3]

index $i$	$i$ -th basis function $\varphi_i$	$\langle \varphi_i, \varphi_i \rangle$
0	1	1
1	$\xi_1$	$\frac{1}{3}$
2	$\xi_2$	$\frac{1}{3}$
3	$\frac{1}{2}(3\xi_1^2 - 1)$	$\frac{1}{5}$
4	$\xi_1 \xi_2$	$\frac{1}{9}$
5	$\frac{1}{2}(3\xi_2^2 - 1)$	$\frac{1}{5}$

### A. Transmission line

In this first example, a lossy microstrip line of length 8 cm is modeled within the frequency range  $[0 - 4]$  GHz. Its cross section is shown in Fig. 2. The copper line has width  $w = 160 \mu\text{m}$ , thickness  $t = 15 \mu\text{m}$  and conductivity  $\sigma = 5.8 \cdot 10^7 \text{ S/m}$ . The dielectric is  $\text{SiO}_2$  of thickness  $h = 180 \mu\text{m}$  with relative permittivity  $\epsilon_r = 3.9$  and loss tangent  $\tan\delta = 0.001$ .

The length and width of the conductor and the dielectric relative permittivity are considered as independent random variables with a uniform PDF, varying within a range of  $\pm 5\%$  with respect to the central value mentioned previously. We note

<sup>1</sup>Based on the fact that  $\int_{-1}^1 P_n(x)^2 dx = 2/(2n+1)$  where  $P_n(x)$  are the Legendre polynomials.

<sup>2</sup>The Mathworks, Inc., Natick

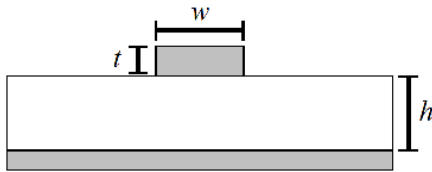


Fig. 2. Example A. Cross section of the lossy microstrip.

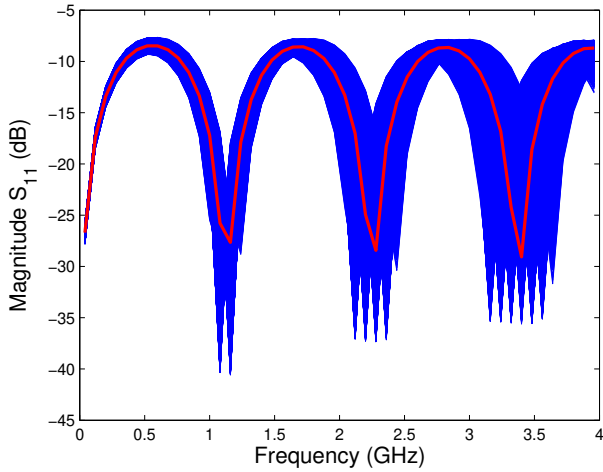


Fig. 3. Example A. Variability of the magnitude of  $S_{11}$ . The thick red line corresponds to the central value for  $L$ ,  $w$  and  $\epsilon_r$ , while the blue lines are the results of MC simulations.

that the choice of a line length as parameter for the variability analysis is particularly meaningful because:

- it causes a shift of the resonances of the microstrip, since a total variation of 0.8 cm in the line length is considered during the variability analysis, see Fig. 3;
- it cannot be modeled using the techniques described in [2]–[4], since they start from a stochastic model of the per-unit-length parameters for the variability analysis.

The scattering parameters are evaluated using a quasi-analytical model [21] over a grid composed of  $4 \times 4 \times 4$  ( $L, w, \epsilon_r$ ) samples for all the random variables and 101 samples for the frequency. The frequency samples are divided in two groups: modeling points (51 samples), used to calculate the state-space representation of the scattering parameters, and validation points (50 samples), used to verify the accuracy of the PC-model with respect to the MC analysis.

The state-space matrices are calculated using the VF algorithm, targeting  $-50$  dB as maximum absolute model error between the scattering parameters and the corresponding *root macromodels* in order to estimate the required number of poles. The PC expansion is calculated using  $P = 2$  and  $M = 9$ , according to (5). In Table II the computational time needed for the MC analysis (performed using 10000 ( $L, w, \epsilon_r$ ) samples for the validation frequencies) and the proposed PC-based technique is reported. Additionally, for the proposed PC method, the computational time needed to calculate the initial samples and to build the polynomial model of the scattering parameters is shown. The comparison in Table II illustrates the significant efficiency gain of the proposed technique.

TABLE II

EXAMPLE A. EFFICIENCY OF THE PROPOSED PC-BASED TECHNIQUE

Technique	Computational time
Monte Carlo Analysis (10000 samples)	152.1 s
PC-based technique	7.43 s
Details PC-based technique	
Initial simulations (64 samples)	0.97 s
PC model scattering parameters	6.46 s

To calculate the port voltages and currents variability, we use a frequency-domain Thévenin voltage source of 1 V with a source impedance of  $50 \Omega$ . The line is also terminated by  $50 \Omega$ .

The proposed PC-based technique has an excellent accuracy compared with the classical MC analysis in computing system variability features, as shown in Figs. 4 - 7. In particular, Figs. 4, 5 show the mean and the standard deviation of the real part of the element  $S_{12}$ , Fig. 6 describes the PDF and the CDF of  $S_{11}$  at 1.24 GHz and Fig. 7 shows the standard deviation of the imaginary part of the current at the output port of the microstrip. Similar results can be obtained for the other entries of the scattering matrix and for the port signals.

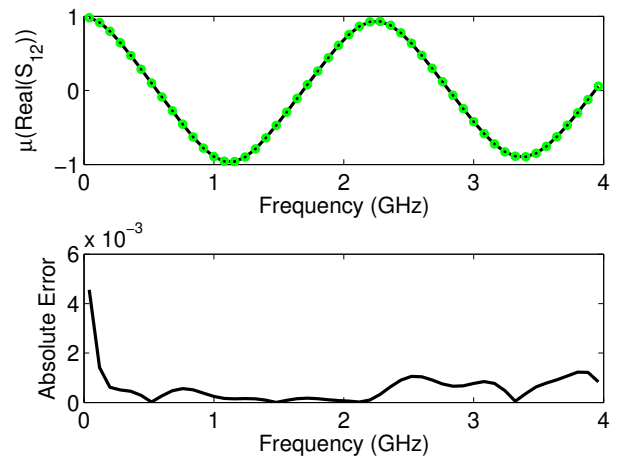


Fig. 4. Example A. The top plot shows a comparison between the mean of the real part of  $S_{12}$  obtained with the MC analysis (full black line) and the proposed PC-based method (green circles: (o)) for the validation frequencies. The lower plot shows the absolute error between the two values.

### B. Double Folded Stub Microstrip Bandstop Filter

In this second example, a double folded stub microstrip bandstop filter [17] has been modeled within the frequency range  $[4.75 - 20.25]$  GHz. Its layout is shown in Fig. 8. The substrate is 0.1270 mm thick with a relative dielectric constant  $\epsilon_r = 9.9$  and a loss tangent  $\tan\delta = 0.003$ . The length

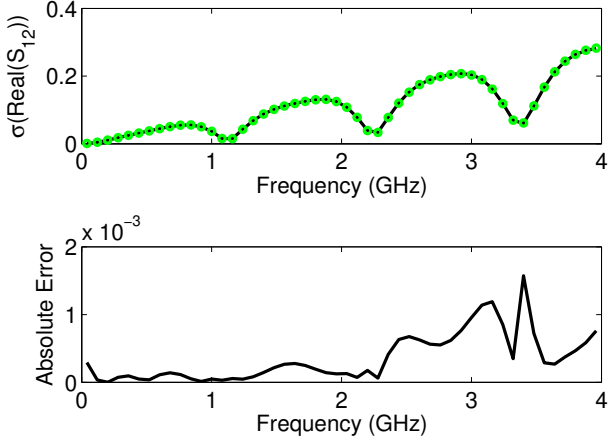


Fig. 5. Example A. The top plot shows a comparison between the standard deviation of the real part of  $S_{12}$  obtained with the MC analysis (full black line) and the proposed PC-based method (green circles:  $\circ$ ) for the validation frequencies. The lower plot shows the absolute error between the two values.

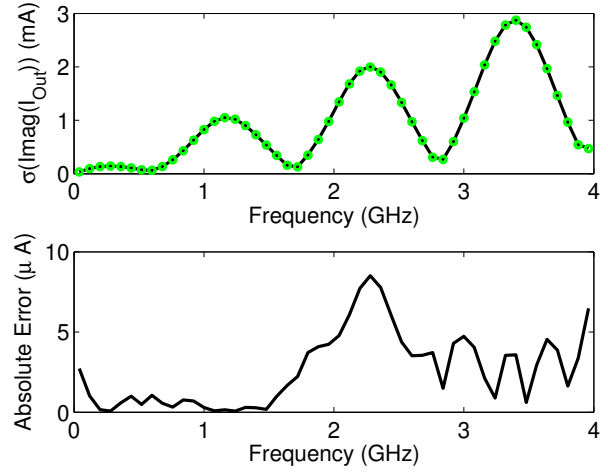


Fig. 7. Example A. The top plot shows a comparison between the standard deviation of the imaginary part of the current at the output port of the microstrip obtained with the MC analysis (full black line) and the proposed PC-based method (green circles:  $\circ$ ) for the validation frequencies. The lower plot shows the absolute error between the two values.

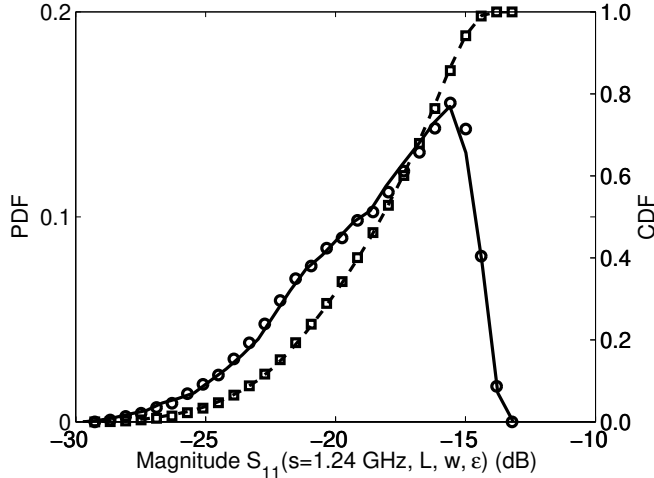


Fig. 6. Example A. PDF and CDF of the magnitude of  $S_{11}$  at 1.24 GHz. Full black line: PDF computed using the novel technique; Dashed black line: CDF computed using the novel technique; Circles ( $\circ$ ): PDF computed using MC technique; Squares ( $\square$ ): CDF computed using MC technique.

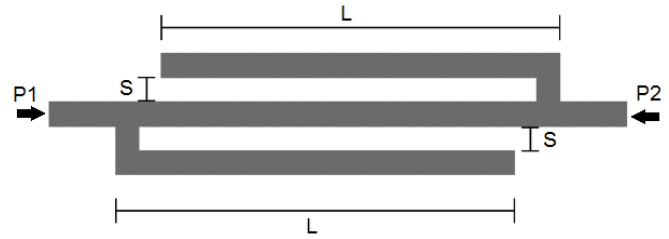


Fig. 8. Example B. Geometry of the double folded stub microstrip bandstop filter.

$L$  and the distance  $S$  are considered independent random variables with a uniform PDF, varying in a range of  $\pm 10\%$  with respect to the central value  $L_0 = 2.1946 \text{ mm}$  and  $S_0 = 0.1219 \text{ mm}$ , respectively. The scattering parameters are evaluated using the program ADS Momentum<sup>3</sup> over a grid composed of  $6 \times 6$  ( $L, S$ ) samples for the geometrical parameters and 62 samples for the frequency. Then, the frequency samples are divided in two groups: modeling points (31 samples) and validation points (31 samples). In this example, the scattering parameters show a high variability with respect to ( $L, S$ ), as shown in Fig. 9.

As in the previous example, VF is used to construct the *root macromodels* for the modeling points, and the accuracy target was again set at  $-50 \text{ dB}$ . The PC expansion is calculated using

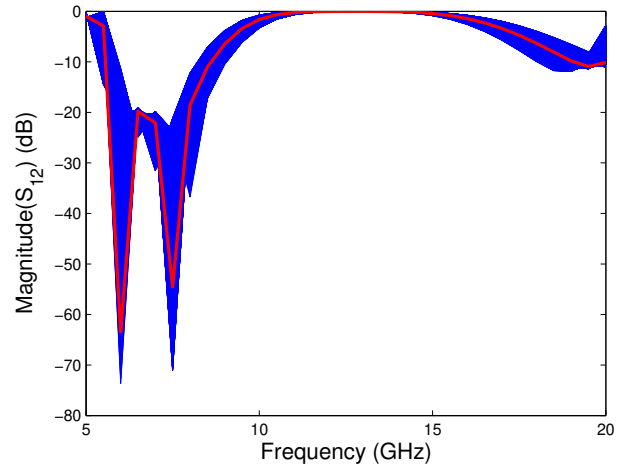


Fig. 9. Example B. Variability of the magnitude of  $S_{12}$ . The thick red line corresponds to the central value for  $S$  and  $L$ , while the blue lines are the results of MC simulations.

<sup>3</sup>Momentum EEsof EDA, Agilent Technologies, Santa Rosa, CA.



$P = 3$  and  $M = 9$ , according to (5).

The comparison between the computational time needed for the MC analysis performed using 10000 ( $L, S$ ) samples for the validation points and the proposed PC-based technique is shown in Table III, demonstrating the efficiency of the proposed PC-based method. In Fig. 10 it is shown an example of the convergence rate of the MC analysis in computing the system variability features; note how the choice of the sample size for the MC analysis affects the accuracy.

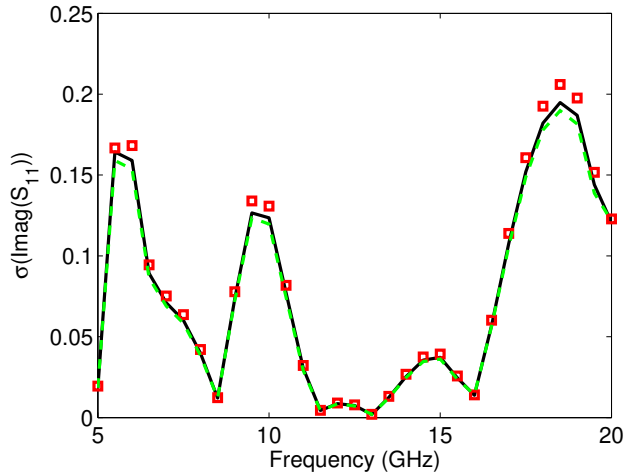


Fig. 10. Example B. Standard deviation of imaginary part of  $S_{11}$  obtained with the MC analysis using different sample size. Full black line: standard deviation computed using 10000 samples; Dashed green line: standard deviation computed using 1000 samples; Squares ( $\square$ ): standard deviation computed using 100 samples.

TABLE III  
EXAMPLE B. EFFICIENCY OF THE PROPOSED PC-BASED TECHNIQUE

Technique	Computational time
Monte Carlo Analysis (10000 samples)	253 h, 22 min, 37.2 s
PC-based technique	54 min 56.88 s
Details PC-based technique	Computational time
Initial EM simulations (36 samples, ADS)	54 min 43.76 s
PC model scattering parameters	13.12 s

In order to evaluate the variability of the port voltages and currents, the filter is excited by a frequency-domain Thévenin voltage source of 1 V with a source impedance of  $50 \Omega$  and the filter is terminated on a  $50 \Omega$  impedance.

Figures 11 - 13 show the accuracy of the proposed PC-based technique compared to the classical MC analysis in computing system variability features. In particular, Figs. 11 and 12 show the mean and the standard deviation of the real part of the element  $S_{22}$ , Fig. 13 describes the PDF and the CDF of  $S_{12}$  at 7.5 GHz and Fig. 14 shows the standard deviation of the imaginary part of the voltage at the output port of the filter.

Similar results can be obtained for all other entries of the scattering matrix and for the port signals.

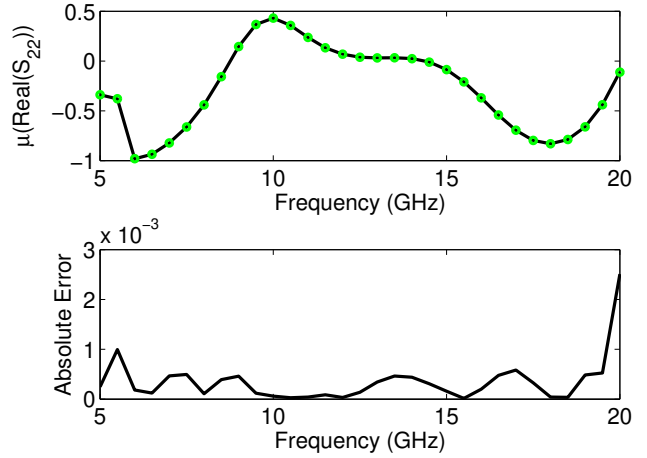


Fig. 11. Example B. The top plot shows a comparison between the mean of the real part of  $S_{22}$  obtained with the MC analysis (full black line) and the proposed PC-based method (green circles:  $(\circ)$ ) for the validation frequencies. The lower plot shows the absolute error between the two values.

## V. CONCLUSIONS

In this paper, an innovative technique for efficient variability analysis of general multiport systems, such as interconnections, filters, connectors, etc., is presented. It is based on the calculation of *root macromodels* of the system transfer functions and on the PC expansion of the corresponding state-space matrices. The approach allows a representation of the transfer function including its statistical properties. This transfer function may be expressed in terms of e.g. scattering, impedance or admittance parameters, as such making it applicable to a large range of systems. The accuracy and efficiency of the proposed method are validated by means of comparison with the standard MC approach, and this for two distinct illustrative examples.

## REFERENCES

- [1] M. S. Eldred, "Recent advance in non-intrusive polynomial-chaos and stochastic collocation methods for uncertainty analysis and design," in *Proc. 50th AIAA/ASME/ASCE/AHS/ASC Structures, Structural Dynamics, and Materials Conference*, Palm Springs, California, May 2009.
- [2] I. S. Stievano, P. Manfredi, F. G. Canavero, "Parameters variability effects on multiconductor interconnects via Hermite polynomial chaos," *IEEE Trans. Compon., Packag., Manuf. Technol.*, vol. 1, no. 8, pp. 1234–1239, Aug. 2011.
- [3] —, "Stochastic analysis of multiconductor cables and interconnects," *IEEE Trans. Electromagn. Compat.*, vol. 53, no. 2, pp. 501–507, May 2011.
- [4] D. Vande Ginste, D. De Zutter, D. Deschrijver, T. Dhaene, P. Manfredi, F. G. Canavero, "Stochastic modeling based variability analysis of on-chip interconnects," *accepted for publication on IEEE Trans. Compon., Packag., Manuf. Technol.*, 2012.
- [5] Q. Su, K. Strunz, "Stochastic circuit modelling with Hermite polynomial chaos," *IET Electronics Letters*, vol. 41, no. 21, pp. 1163–1165, Oct. 2005.
- [6] K. Strunz, Q. Su, "Stochastic formulation of SPICE-type electronic circuit simulation using polynomial chaos," *ACM Transactions on Modeling and Computer Simulation*, vol. 18, no. 4, pp. 501–507, Sep. 2008.

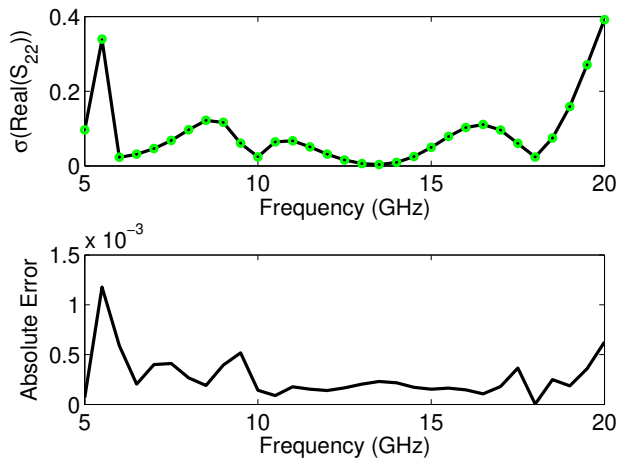


Fig. 12. Example B. The top plot shows a comparison between the standard deviation of the real part of  $S_{22}$  obtained with the MC analysis (full black line) and the proposed PC-based method (green circles:  $\circ$ ) for the validation frequencies. The lower plot shows the absolute error between the two values.

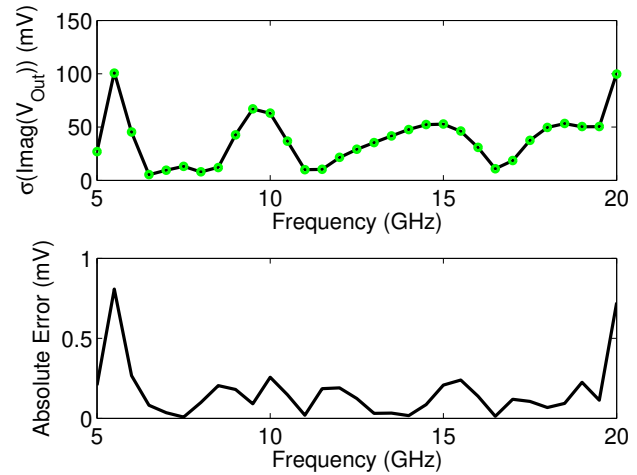


Fig. 14. Example B. The top plot shows a comparison between the standard deviation of the imaginary part of the voltage at the output port of the filter obtained with the MC analysis (full black line) and the proposed PC-based method (green circles:  $\circ$ ) for the validation frequencies. The lower plot shows the absolute error between the two values.

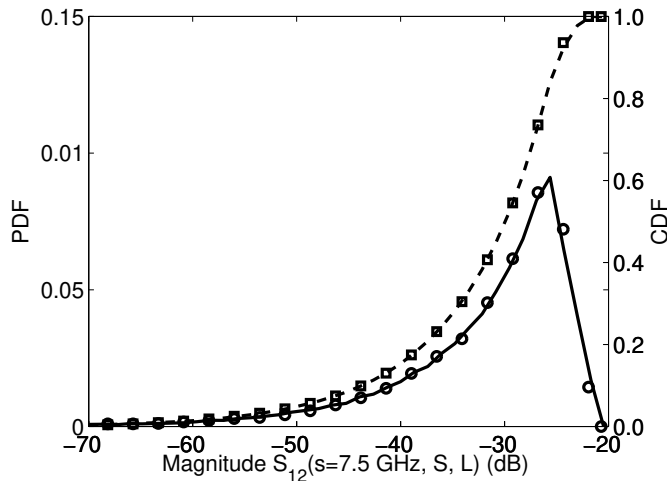


Fig. 13. Example B. PDF and CDF of the magnitude of  $S_{12}$  at 7.5 GHz. Full black line: PDF computed using the novel technique; Dashed black line: CDF computed using the novel technique; Circles ( $\circ$ ): PDF computed using MC technique; Squares ( $\square$ ): CDF computed using MC technique.

- [7] B. Gustavsen and A. Semlyen, "Rational approximation of frequency domain responses by vector fitting," *IEEE Trans. Power Del.*, vol. 14, no. 3, pp. 1052–1061, Jul. 1999.
- [8] B. Gustavsen, "Improving the pole relocating properties of vector fitting," *IEEE Trans. Power Del.*, vol. 21, no. 3, pp. 1587–1592, Jul. 2006.
- [9] D. Deschrijver, M. Mrozowski, T. Dhaene, and D. De Zutter, "Macro-modeling of multiport systems using a fast implementation of the vector fitting method," *IEEE Microw. Wireless Compon. Lett.*, vol. 18, no. 6, pp. 383–385, Jun. 2008.
- [10] W. Schoutens, *Stochastic Processes and Orthogonal Polynomials*. Springer, 2000.
- [11] J. A. S. Witteveen and H. Bijl, "Modeling Arbitrary Uncertainties Using Gram-Schmidt Polynomial Chaos," in *Proc. 44th AIAA Aerospace Sciences Meeting and Exhibit*, no. AIAA-2006-0896, Palm Springs, California, Jan. 2006.
- [12] D. Xiu and G.M. Karniadakis, "The Wiener-Askey polynomial chaos for stochastic differential equations," *SIAM J. Sci. Comput.*, vol. 24, no. 2, pp. 619–644, Apr. 2002.
- [13] C. Soize and R. Ghanem, "Physical systems with random uncertainties:

Chaos representations with arbitrary probability measure," *SIAM J. SCI. COMPUT.*, vol. 26, no. 2, pp. 395–410, Jul. 2004.

- [14] A. Der Kiureghian and P. L. Liu, "Structural reliability under incomplete probability information," *J. Eng. Mech., ASCE*, vol. 112, no. 1, pp. 85–104, 1986.
- [15] M. Loeve, *Probability Theory*, 4th ed. Springer-Verlag, 1977.
- [16] A. Papoulis, *Probability, Random Variables and Stochastic Processes*. McGraw-Hill College, 1991.
- [17] F. Ferranti, L. Knockaert and T. Dhaene, "Parameterized S-parameter based macromodeling with guaranteed passivity," *IEEE Microw. Wireless Compon. Lett.*, vol. 19, no. 10, pp. 608–610, Oct. 2009.
- [18] F. Ferranti, L. Knockaert, T. Dhaene and Giulio Antonini, "Passivity-preserving parametric macromodeling for highly dynamic tabulated data based on Lur'e equations," *IEEE Trans. Microw. Theory Tech.*, vol. 58, no. 12, pp. 3688–3696, Dec. 2010.
- [19] E. G. Gilbert, "Controllability and observability in multivariable control systems," *SIAM Journal on Control*, vol. 2, no. 1, pp. 128–151, 1963.
- [20] D. M. Pozar, *Microwave Engineering (Addison-Wesley Series in Electrical and Computer Engineering)*. Addison-Wesley, 1990.
- [21] K. C. Gupta, R. Garg, I. Bahl, and P. Bhartia, *Microstrip Lines and Slotlines*, 2nd ed. Artech House, Inc., Norwood, MA, 1996.



**Domenico Spina** received the M.S. degree (summa cum laude) in electronic engineering from Università degli Studi dell'Aquila, L'Aquila, Italy, in 2010. He is currently pursuing the Ph.D. degree with the Department of Information Technology, Ghent University, Ghent, Belgium. His current research interests include modeling and simulation, system identification, microwave engineering, sensitivity and uncertainty analysis.



**Francesco Ferranti** (M'10) received the B.S. degree (summa cum laude) in electronic engineering from Università degli Studi di Palermo, Palermo, Italy, the M.S. degree (summa cum laude and honors) in electronic engineering from Università degli Studi dell'Aquila, L'Aquila, Italy, and the Ph.D. degree in electrical engineering from Ghent University, Ghent, Belgium, in 2005, 2007, and 2011, respectively. He is currently a Post-Doctoral Research Fellow with the Department of Information Technology, Ghent University, Ghent, Belgium. His current research

interests include parametric macromodeling, parameterized model order reduction, electromagnetic compatibility, numerical modeling, and system identification.



**Tom Dhaene** (M'00–SM'05) was born in Deinze, Belgium, on June 25, 1966. He received the Ph.D. degree in electrotechnical engineering from the Ghent University, Ghent, Belgium, in 1993. He was a Research Assistant with the Department of Information Technology, University of Ghent, Ghent, Belgium, from 1989 to 1993, where his research focused on different aspects of full-wave electromagnetic circuit modeling, transient simulation, and time-domain characterization of high-frequency and high-speed interconnections. In 1993, he joined the

Electronic Design Automation Company Alphabit (now part of Agilent), Santa Clara, CA. He was one of the key developers of the planar EM simulator ADS Momentum. In September 2000, he joined the Department of Mathematics and Computer Science, University of Antwerp, Antwerp, Belgium, as a Professor. Since October 2007, he has been a Full Professor in the Department of Information Technology, Ghent University, Ghent, Belgium. He is the author or co-author of more than 250 peer reviewed papers and abstracts in international conference proceedings, journals, and books. He holds five U.S. patents.



**Luc Knockaert** (M'81–SM'00) received the M.Sc. Degree in physical engineering, another M.Sc. Degree in telecommunications engineering, and the Ph.D. degree in electrical engineering from Ghent University, Ghent, Belgium, in 1974, 1977 and 1987, respectively. He was working in the North–South Cooperation and in development projects with the Universities of the Democratic Republic of Congo and Burundi from 1979 to 1984 and from 1988 to 1995. He is currently with the Interdisciplinary Institute for BroadBand Technologies and a Professor

with the Department of Information Technology, Ghent University, Ghent, Belgium. He is the author or co-author of more than 100 papers published in international journals and conference proceedings. His current research interests include the application of linear algebra and adaptive methods in signal estimation, model order reduction, and computational electromagnetics. Prof. Knockaert is a member of the Mathematical Association of America and the Society for Industrial and Applied Mathematics.



**Giulio Antonini** (M'94–SM'05) received the Laurea degree (summa cum laude) in electrical engineering from Università degli Studi dell'Aquila, L'Aquila, Italy, in 1994, and the Ph.D. degree in electrical engineering from the University of Rome "La Sapienza", Rome, Italy, in 1998. He has been with the Department of Electrical Engineering, UAQ EMC Laboratory, University of L'Aquila, L'Aquila, Italy, since 1998, where he is currently an Associate Professor. He has given keynote lectures and chaired several special sessions at international conferences.

He holds one European patent. He has authored or coauthored more than 180 technical papers and two book chapters. His current research interests include electromagnetic compatibility analysis, numerical modeling, and signal integrity for high-speed digital systems. Dr. Antonini was the recipient of the IEEE TRANSACTIONS ON ELECTROMAGNETIC COMPATIBILITY Best Paper Award in 1997, the CST University Publication Award in 2004, and the IBM Shared University Research Award in 2004, 2005, and 2006. In 2006, he received a Technical Achievement Award from the IEEE EMC Society "for innovative contributions to computational electromagnetic on the Partial Element Equivalent Circuit technique for EMC applications". He received the Institution of Engineering and Technology – Science, Measurement and Technology Best Paper Award in 2008. He is the Chair of the IEEE EMC Italy Chapter, the Chair of the TC–10 Committee and member of the TC–9 Committee of the IEEE EMC Society. He serves as member of the Editorial Board of the IET Science, Measurements, and Technology. He also serves as a reviewer for a number of IEEE journals.



**Dries Vande Ginste** (M'07) was born in 1977. He received the M.S. and Ph.D. degrees in electrical engineering from Ghent University, Ghent, Belgium, in 2000 and 2005, respectively. He is currently an Assistant Professor with the Department of Information Technology, Electromagnetics Group, Ghent University. In 2004, he was a Visiting Scientist with the Department of Electrical and Computer Engineering, University of Illinois at Urbana–Champaign, Urbana. In 2011, he was a Visiting Professor with the Dipartimento di Elettronica, EMC

Group, Politecnico di Torino, Torino, Italy. His current research interests include computational electromagnetics, electromagnetic compatibility, signal and power integrity, and antenna designs. Dr. Vande Ginste received the International Union of Radio Science (URSI) Young Scientist Award at the 2011 URSI General Assembly and Scientific Symposium.